Supplementary Figure 1

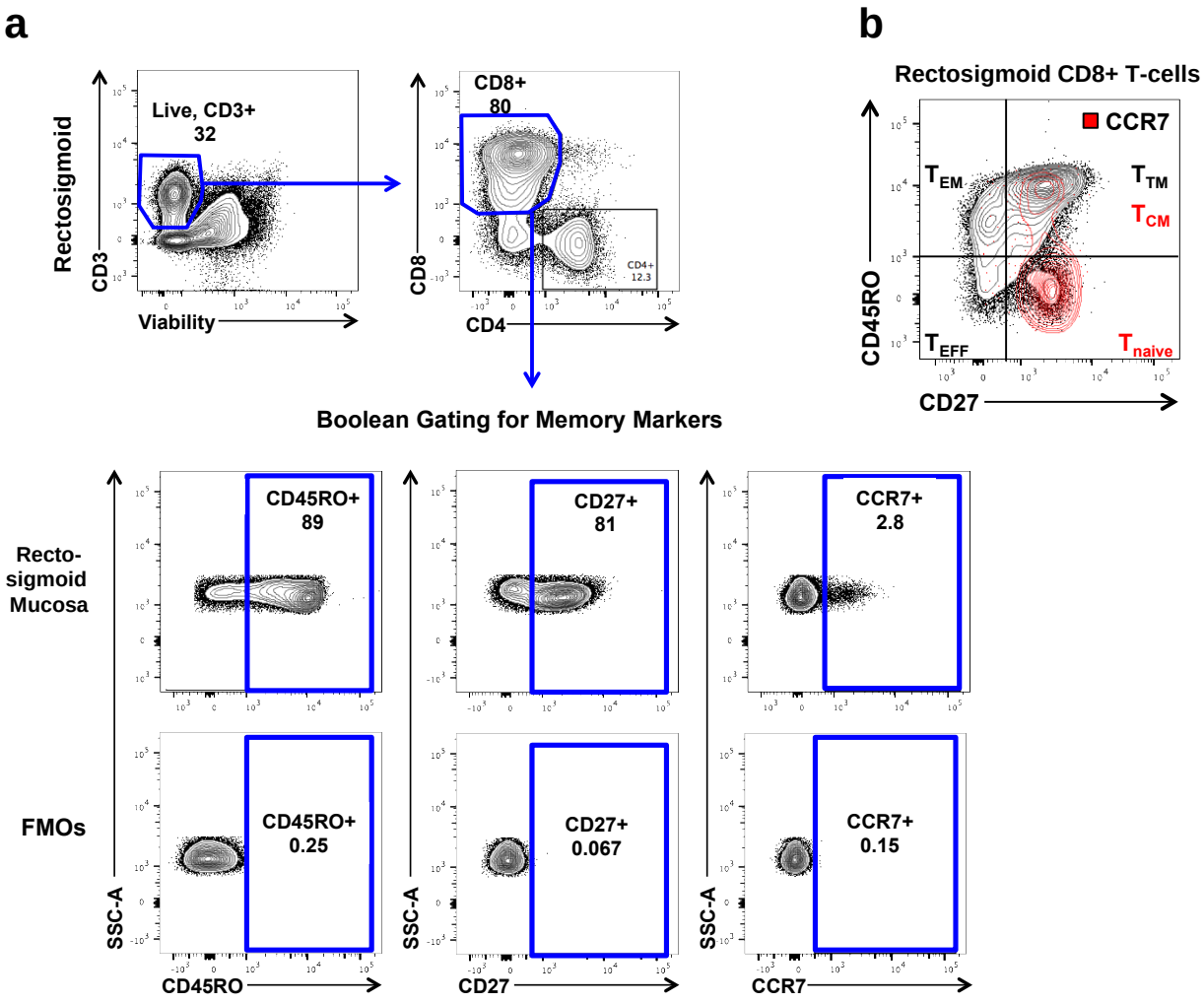

Supplementary Figure 1. Gating strategy for CD8$^+$ T-cell memory subsets in the human rectosigmoid mucosa. **(a)** Representative flow cytometry plot showing gating strategy used to identify live, CD3$^+$, CD8$^+$ T-cell memory subsets in the mucosa. Memory subsets were defined by first establishing positive gates for each memory marker within the live, CD3$^+$, CD8$^+$ T-cell population followed by Boolean gating to define memory subsets as follows: naïve (T_{naive} CD45RO$^-$CD27$^+$CCR7$^+$), central memory (T_{CM} CD45RO$^+$CD27$^+$CCR7$^+$), transitional memory (T_{TM} CD45RO$^+$CD27$^+$CCR7$^-$), effector memory (T_{EM} CD45RO$^+$CD27$^-$CCR7$^-$), and effector (T_{EFF} CD45RO$^-$CD27$^-$CCR7$^-$). **(b)** Representative flow cytometry plot displaying the co-expression of CD45RO, CD27, and CCR7 in rectosigmoid CD8$^+$ T-cells.

Supplementary Figure 2

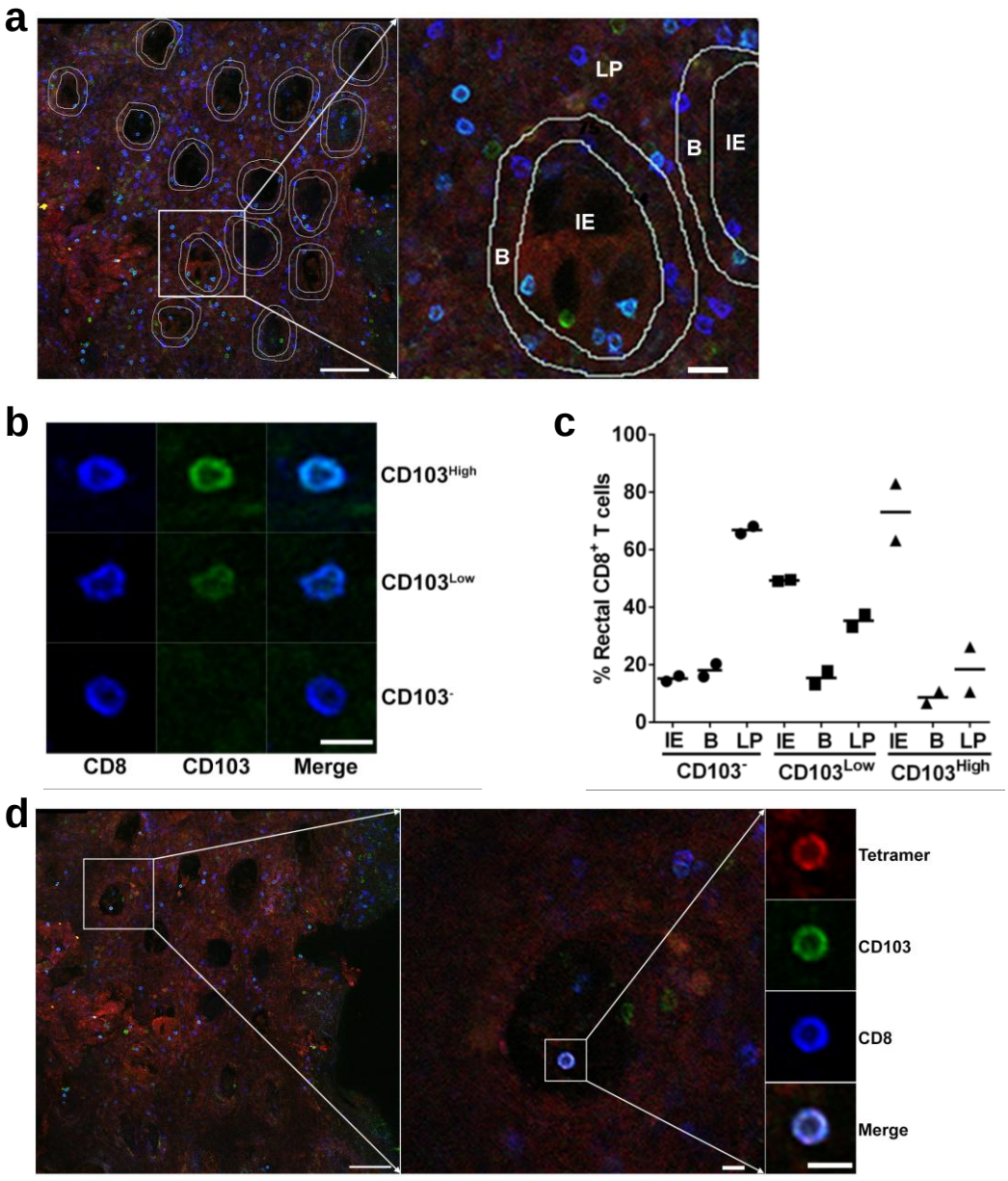

Supplementary Figure 2. Distribution of CD103^{-}, CD103^{Low} and CD103^{High} CD8^{+} T cells in rectosigmoid mucosa of HIV-1 controllers. **(a)** Representative tissue section illustrating delineation of compartments within the mucosa, including crypts with intraepithelial lymphocytes (IE), border areas (B) and lamina propria (LP). Stained with HLA-B*57/Gag QW9 tetramers (red), CD8 antibodies (blue) and CD103 antibodies (green), the red background signal from tetramers was used to help delineate crypts. Confocal images were collected with a 20X objective. The scale bar indicates 100 µm (left) and 20 µm (right). **(b)** Representative rectosigmoid CD8^{+} T cells (blue) from that were CD103^{-}, CD103^{Low} and CD103^{High}. Scale bar indicates 10 µm. **(c)** Percentage of CD103^{-}, CD103^{Low} and CD103^{High} CD8^{+} T cells in different anatomic compartments. **(d)** Representative epithelial CD103^{+} HIV-specific CD8^{+} T cell in rectosigmoid mucosa. Scale bar indicates 100, 10, and 10 µm, respectively.

Supplementary Figure 3

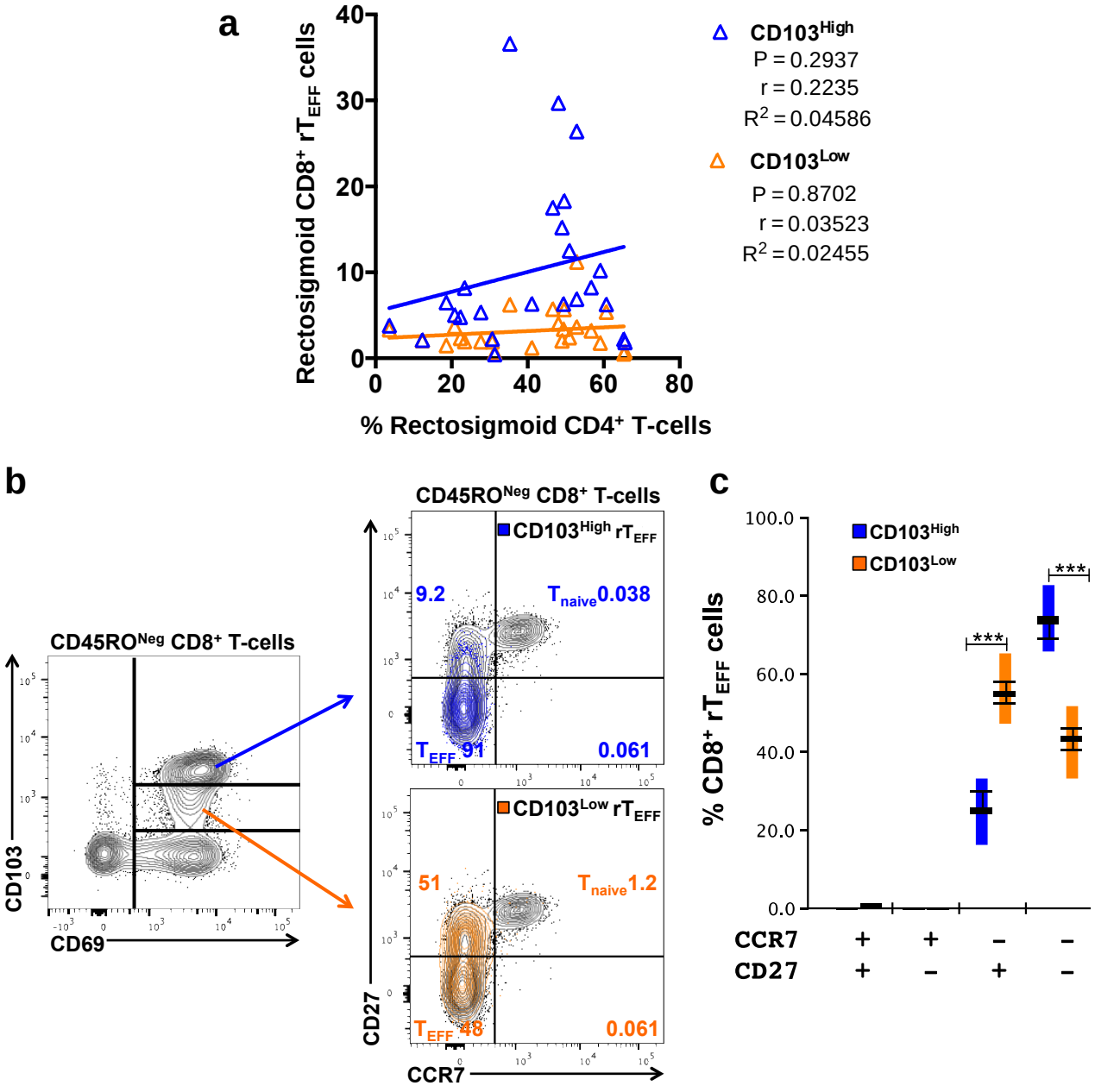

Supplementary Figure 3. Associations between CD103^{High} and CD103^{Low} CD8^{+} rT$_{EFF}$, expression of CD27 and abundance of rectosigmoid CD4^{+} T-cells. **(a)** No significant correlations were observed between the percentage of rectosigmoid CD103^{High} or CD103^{Low} CD8^{+} rT$_{EFF}$ and percentage of rectosigmoid CD4^{+} T-cells. **(b)** Representative flow plot showing differences in expression of CD27 and CCR7 between CD103^{High} and CD103^{Low} CD8^{+} rT$_{EFF}$ cells. **(c)** Frequencies of CD103^{High} and CD103^{Low} CD8^{+} rT$_{EFF}$ expressing CD27 and CCR7 in all study participants. Non-parametric Spearman correlation and linear regression were used to calculate associations. Co-expression analysis was generated using SPICE software. Vertical bars represent interquartile ranges, horizontal bars represent medians, whiskers indicate standard error of the mean with level of significance: * P <0.05, ** P <0.01, *** P <0.001.

Supplementary Figure 4

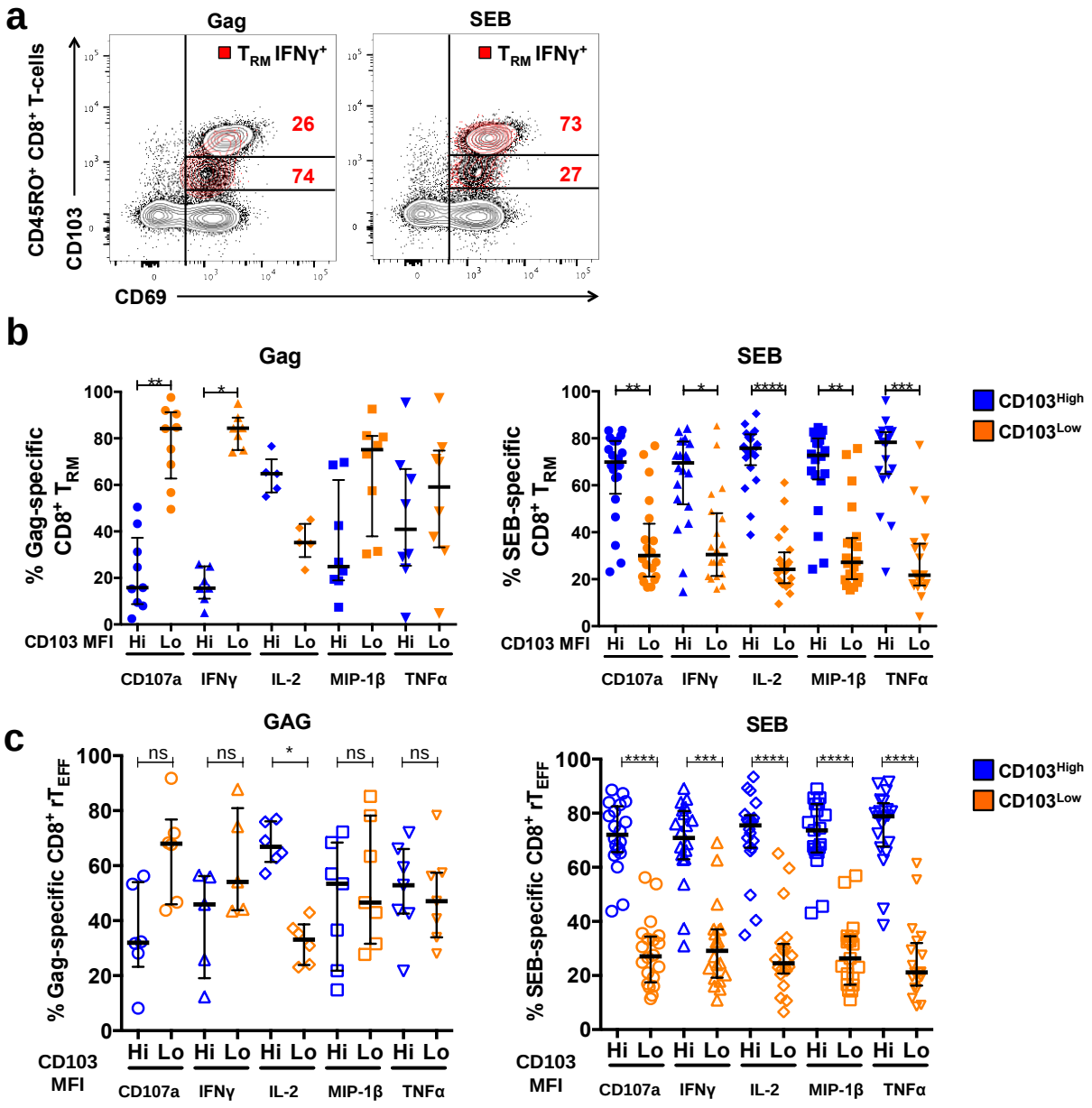

Supplementary Figure 4. Functionality and CD103 median fluorescence intensity (MFI) of $CD8^+$ T_{RM} and rT_{EFF} responding to antigenic stimulation. **(a)** Representative flow cytometry plot showing CD103 fluorescence intensity of rectosigmoid $CD8^+$ T_{RM} producing IFNγ in response to HIV-1 Gag-peptide pool (red, left) or SEB (red, right). **(b)** Differences in CD103 MFI among individual responses and between Gag- and SEB-responding $CD8^+$ T_{RM} in a consolidated group of study participants. (c) Differences in CD103 MFI between individual responses and between Gag and SEB-responding $CD8^+$ rT_{EFF}. Response data were generated using Boolean gating within live, $CD3^+$, $CD8^+$, $CD45RO^+$ or $CD45RO^{Neg}$, $CD103^+CD69^+S1PR1^-$ cells. Horizontal bars represent medians, whiskers indicate interquartile ranges with level of significance indicated as follows: * P <0.05, ** P <0.01, *** P <0.001, **** P <0.0001.

Supplementary Figure 5

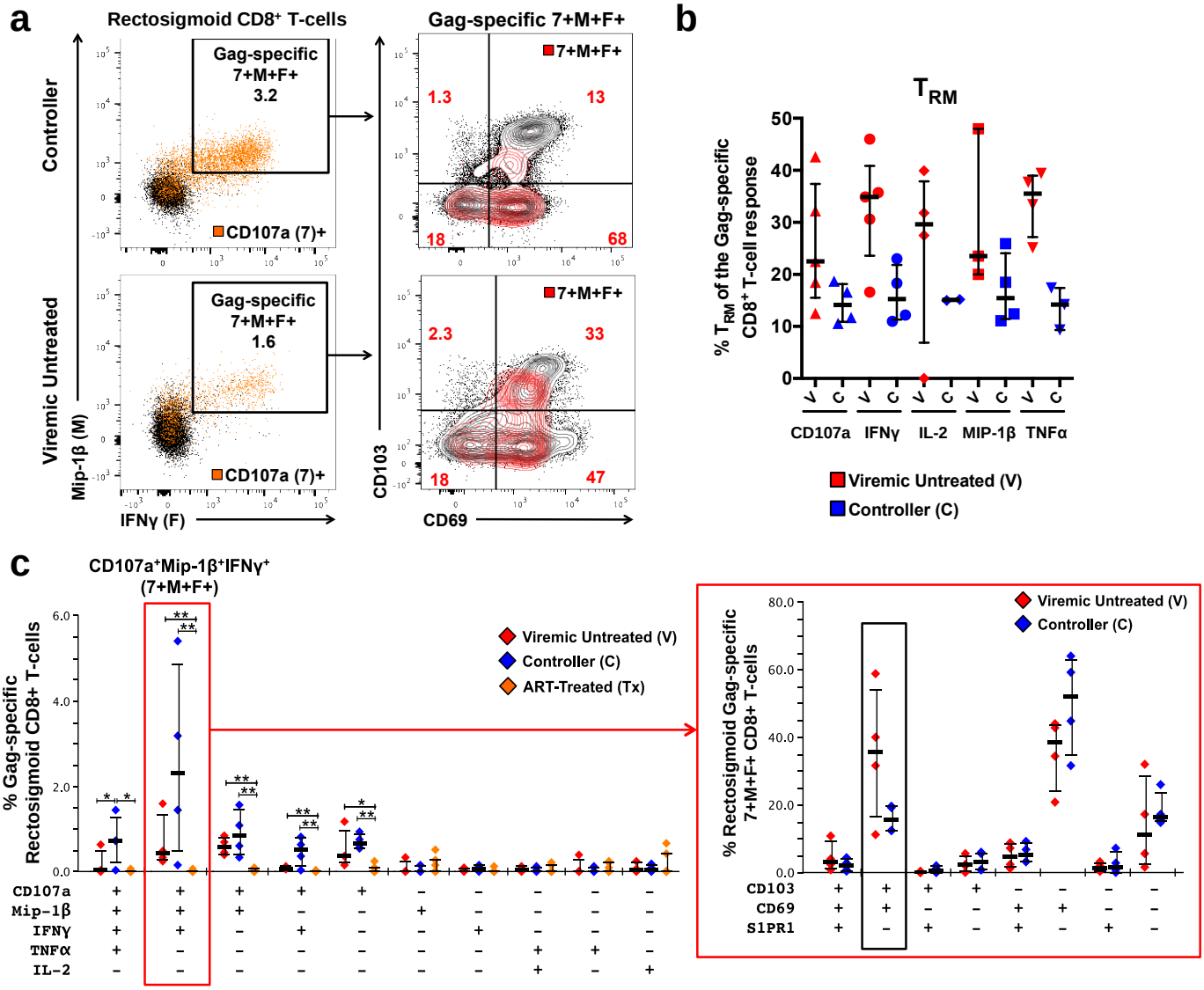

Supplementary Figure 5. Contribution of tissue-resident CD8$^+$ T-cells to the total rectosigmoid CD8$^+$ T-cell HIV-1 Gag-specific response varies across disease status. **(a)** Representative flow cytometry plot showing differences in CD103 and CD69 expression on rectosigmoid Gag-specific CD107a$^+$MIP-1β$^+$IFNγ$^+$ (7$^+$M$^+$F$^+$) CD8$^+$ T-cells between an HIV-1$^+$ controller (top) and an HIV-1$^+$ viremic participant not on ART (bottom). **(b)** Difference in the contribution of CD8$^+$ T_{RM} to individual rectosigmoid Gag-specific CD8$^+$ T-cell responses between controllers and viremic individuals not on ART. **(c)** Difference in the expression of CD103, CD69, and S1PR1 on rectosigmoid Gag-specific CD107a$^+$MIP-1β$^+$IFNγ$^+$ (7$^+$M$^+$F$^+$) CD8$^+$ T-cells between controllers and viremic participants not on ART. Trends were conserved across all polyfunctional subsets analyzed (data not shown). Co-expression analysis was generated using SPICE software. Horizontal bars represent medians, whiskers indicate interquartile ranges with the level of significance indicated with asterisks: * P <0.05, ** P <0.01.

Supplementary Figure 6

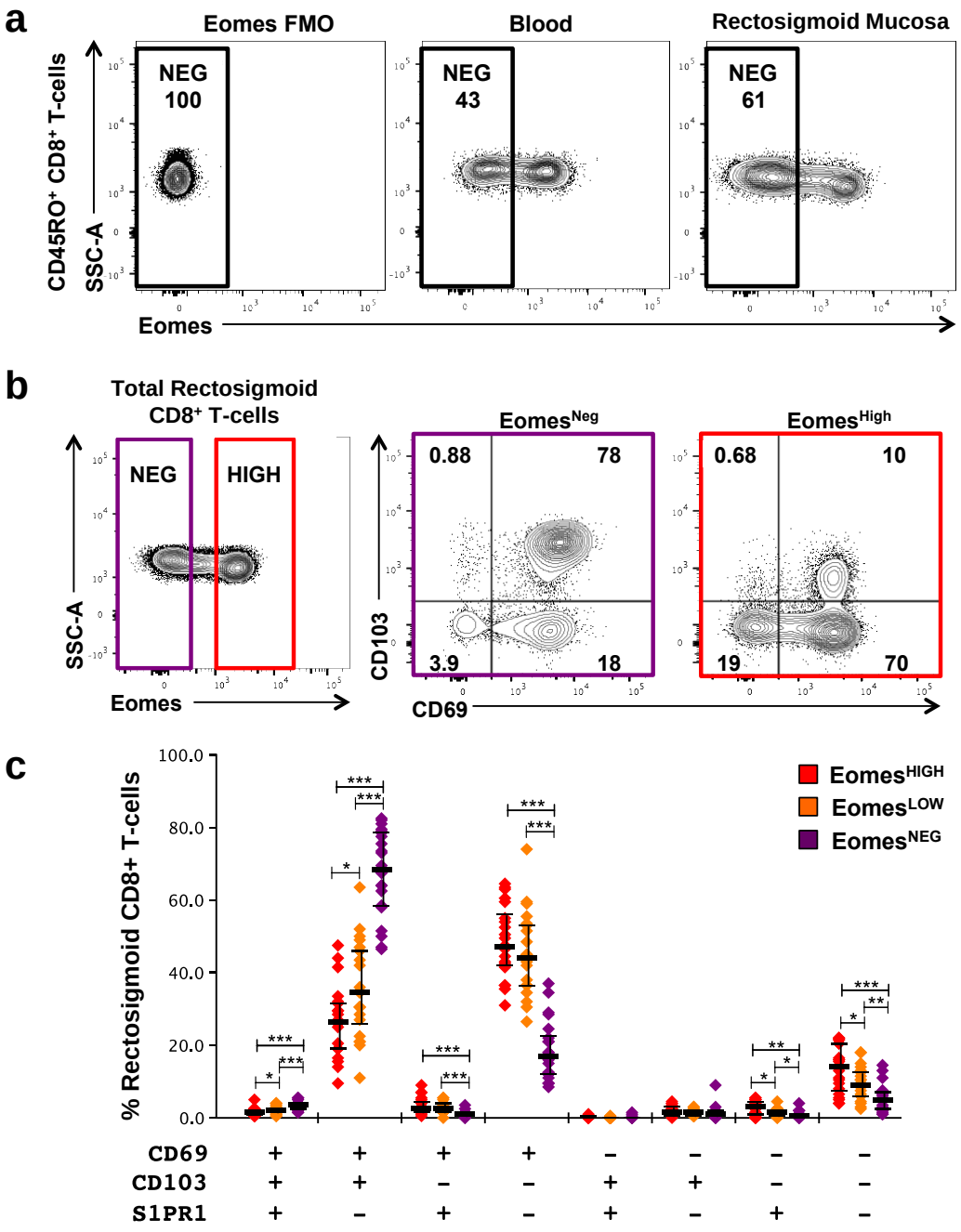

Supplementary Figure 6. Expression of Eomesodermin (Eomes) in rectosigmoid CD8$^+$ T-cells **(a)** Representative staining of blood and rectosigmoid CD45RO$^+$ CD8$^+$ T-cells gated using an Eomes fluorescence minus one control (FMO). **(b)** Representative expression of CD103 and CD69 on Eomes^{High} and Eomes^{Neg} rectosigmoid CD8$^+$ T-cells. **(c)** Co-expression of CD103, CD69, and S1PR1 on Eomes$^{High/Low/Neg}$ rectosigmoid CD8$^+$ T-cells in a group of chronically HIV-1$^+$ and seronegative participants. Whiskers indicate interquartile ranges. Level of significance is indicated with asterisks: * P <0.05, ** P <0.01, *** P <0.001.

Supplementary Figure 7

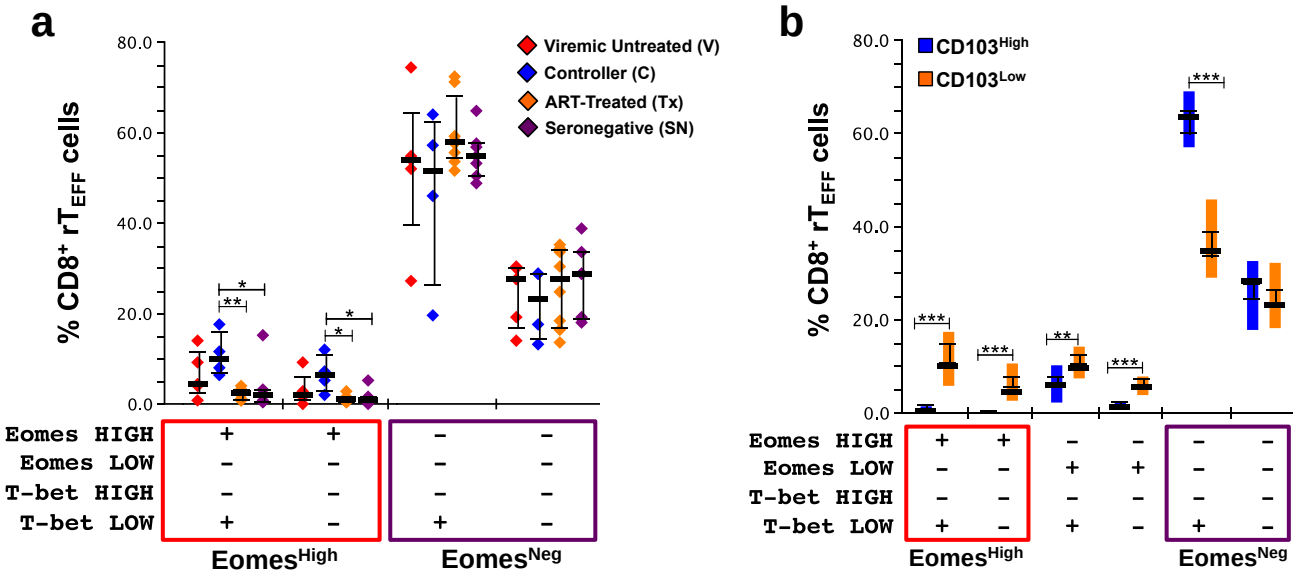

Supplementary Figure 7. Eomes expression in rectosigmoid $CD8^+$ rT_{EFF} varies with HIV-1 disease status and CD103 expression intensity. **(a)** Differences in frequency of $Eomes^{High}$ and $Eomes^{Neg}$ rectosigmoid $CD8^+$ rT_{EFF} across HIV-1 disease status. **(b)** Difference in expression of Eomes and T-bet between $CD103^{High}$ and $CD103^{Low}$ rectosigmoid $CD8^+$ rT_{EFF} cells. Co-expression analyses were generated using SPICE software. Horizontal bars represent medians. In **(a)** whiskers indicate interquartile ranges; in **(b)** vertical bars represent interquartile ranges and whiskers indicate standard error of the mean. Level of significance is indicated with asterisks: * P <0.05, ** P <0.01, *** P <0.001.

Supplementary Figure 8

a

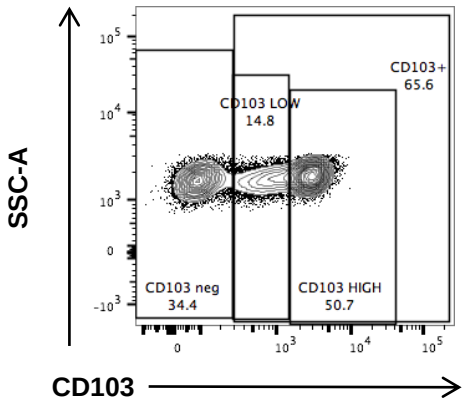

b

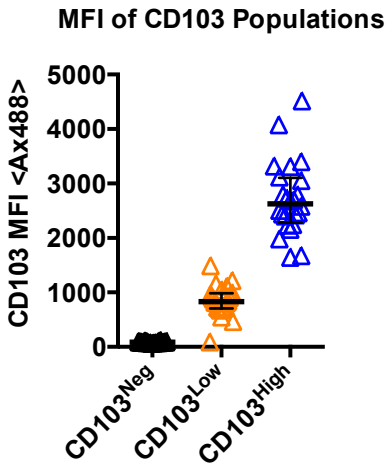

c

HIV Status	Sample	CD103Neg MFI	CD103Low MFI	CD103High MFI	Δ High and Low CD103 MFI	Median Δ	Mean Δ
V	3611	88.2	845	2508	2.968047337		
V	3675	76.5	1044	3318	3.17816092		
V	3610	84.6	707	2158	3.052333805		
V	1748	76.3	908	2725	3.001101322		
V	1476	90.7	1112	3398	3.055755396	3.052333805	3.051079756
C	1247	73.6	705	2697	3.825531915		
C	1788	62.7	465	1980	4.258064516		
C	1737	82.1	963	3052	3.169262721		
C	1270	70	876	2459	2.807077626	3.497397318	3.514984194
Tx	3672	105	811	2677	3.300863132		
Tx	2013	90.8	687	2237	3.256186317		
Tx	2411	73.6	671	1674	2.494783905		
Tx	1672	96.4	736	2793	3.794836957		
Tx	2447	97.5	818	2242	2.740831296		
Tx	1631	88.8	991	3119	3.147325933		
Tx	1103	97.6	725	2789	3.846896552		
Tx	3629	116	1156	3311	2.864186851	3.201756125	3.180738868
SN	3722	101	962	2581	2.682952183		
SN	1811	91.4	834	2401	2.878896882		
SN	6557	79.1	1491	4079	2.73574782		
SN	6523	77.1	812	2441	3.006157635		
SN	6560	82.4	917	2424	2.643402399		
SN	6532	82.6	548	1644	3		
SN	6561	84.1	1215	4513	3.714403292	2.878896882	2.951651459
						Total Median	Total Mean
						3.02924572	3.142616946

Supplementary Figure 8. The figure shows gating to distinguish between CD103neg, low and high populations. **(a)** Representative sample of rectosigmoid $CD8^+$ T-cells with side scatter on the y-axis and CD103 on the x-axis. Sample shown is from an $HIV\text{-}1^+$ viremic individual not on ART. **(b)** Summary of CD103 median fluorescence intensity (MFI) for negative, low and high gates, as detailed in the Table. **(c)** List of all samples analyzed, with MFI for CD103 negative, low and high gates. The median difference in MFI (ΔMFI) between high and low CD103 gates for all samples was 3.02.